Neuro-Oncology

*Neuro-Oncology* 17(12), 1578–1588, 2015
doi:10.1093/neuonc/nov060
Advance Access date 25 May 2015

# Transcriptional upregulation of microtubule-associated protein 2 is involved in the protein kinase A-induced decrease in the invasiveness of glioma cells

**Yuxi Zhou†, Sihan Wu†, Chaofeng Liang†, Yuan Lin, Yan Zou, Kai Li, Bingzheng Lu, Minfeng Shu, Yijun Huang, Wenbo Zhu, Zhuang Kang, Dong Xu, Jun Hu, and Guangmei Yan**

*Department of Pharmacology, Zhongshan School of Medicine, Sun Yat-Sen University, Guangzhou, China (Y.Z., S.W., Y.L., K.L., B.L., M.S., Y.H., W.Z., D.X., J.H., G.Y.); Department of Neurosurgery, The Third Affiliated Hospital of Sun Yat-sen University, Guangzhou, China (C.L.); Department of Imaging, The Third Affiliated Hospital of Sun Yat-sen University, Guangzhou, China (Y.Z., Z.K.); Department of Microbiology, Zhongshan School of Medicine, Sun Yat-Sen University, Guangzhou, China (J.H.)*

**Corresponding Authors:** Jun Hu, PhD, Department of Pharmacology & Department of Microbiology, Zhongshan School of Medicine, Sun Yat-Sen University, Guangzhou 510080 (hujun@mail.sysu.edu.cn); Dong Xu, MD, Department of Pharmacology, Zhongshan School of Medicine, Sun Yat-Sen University, Guangzhou 510080 (xudong@mail.sysu.edu.cn).

†These authors contributed equally to this work.

***Background.*** Malignant glioma is the most lethal primary tumor of the central nervous system, with notable cell invasion causing significant recurrence. Suppression of glioma invasion is very important for improving clinical outcomes. Drugs that directly disrupt the cytoskeleton have been developed for this purpose; however, drug resistance and unsatisfactory selectivity have limited their clinical use. Previously, we reported that protein kinase A (PKA, also known as cyclic-AMP dependent protein kinase) activation induced the differentiation of glioma cells.

***Methods.*** We used several small molecular inhibitors and RNA interference, combined with wound healing assays, Matrigel transwell assay, and microscopic observation, to determine whether activation of the PKA pathway could inhibit the invasion of human glioma cells.

***Results.*** Activation of PKA decreased the invasion of glioma cells. The mechanism operated via transcriptional upregulation of microtubule-associated protein 2 (MAP2), which was activated by the PKA pathway and led to ossification of microtubule dynamics via polymerization of tubulin. This resulted in morphological changes and a reduction in glioma cell invasion. Furthermore, chromosome immunoprecipitation and quantitative real-time polymerase chain reaction showed that signal transducer and activator of transcription 3 (STAT3) is involved in the transcriptional upregulation of MAP2.

***Conclusion.*** Our findings suggested that PKA may represent a potential target for anti-invasion glioma therapy and that the downstream modulators (eg, STAT3/MAP2) partially mediate the effects of PKA.

**Keywords:** cAMP/PKA pathway, invasion, malignant glioma, MAP2, microtubule.

Malignant gliomas, including glioblastoma (GBM) and anaplastic astrocytoma (AA), are the most common and lethal primary tumors of the CNS. Although considerable progress has been made in developing therapies, gliomas remain incurable because of cell invasion. Furthermore, cell invasion is the major cause of tumor recurrence.[1–4]

Invasion of brain tumor cells is thought to be a multistep process. Tumor cells first initiate detachment from their primary adhesion sites. The tumor cells then modify the receptor-mediated adhesion of some extracellular matrix proteins in adjacent sites, followed by degradation of matrix by proteases that are secreted by cancer cells. Tumor cells then migrate to distant sites in normal brain tissue.[5] Migration is the obvious crucial step in the complex process of tumor cell invasion.

Cytoskeletal microtubules are essential for cell migration.[6] Microtubules are dynamically unstable during migration, driving the cell forward into 2 phases of growth and shrinkage.[7,8] Various microtubule-associated proteins (MAPs) regulate the homeostasis of microtubules. MAP2 binds to and increases the rigidity of microtubules. MAP2 plays an important role in

*Received 18 September 2013; accepted 14 March 2015*

the formation of dendritic protrusions in astrocytes and oligodendrocytes.[9] The main forms of MAP2 are low–molecular-weight MAP2 (MAP2c and MAP2d), which are relatively short, and high–molecular-weight MAP2 (MAP2a and MAP2b), which have longer projection domains.[10,11]

Interrupting the depolymerization or polymerization of microtubules (also known as microtubular dynamics interruption) inhibits the motility of tumor cells, thus stopping invasion. Certain drugs such as vinca alkaloids and taxanes, which directly target microtubules, are effective in the treatment of various malignancies. However, their clinical application is limited by resistance developed by cancer cells or undesired toxicities resulting from their inability to target the cancer cells.[12–14] To circumvent these problems, targeting the cancer-specific microtubules' regulation machinery, instead of the microtubules themselves, may represent a therapeutic option. Gliomas express almost no MAP2.[15,16] However, whether MAP2 is a suitable target for anti-invasion therapy for glioma remains to be determined.

Previously, we reported that the PKA activator cholera toxin is capable of inducing differentiation-like morphological changes in glioma cells.[17] Other PKA activators such as N6,2′-O-dibutyryladenosine 3′,5′-cyclic monophosphate (dbcAMP) and forskolin can also induce similar morphological changes in glioma cells.[17–19] However, the effects of the PKA activators on cancer cell invasion and the underlined molecular mechanisms remain largely unknown.

In the present study, we found that human glioma cell lines DBTRG-05MG and A172, as well as human GBM primary cultures, showed marked morphological changes after treatment with different PKA activators. Activation of the PKA pathway inhibited the invasion of C6, DBTRG-05MG and A172 glioma cells by increasing the stability of microtubules. Furthermore, transcriptional upregulation of MAP2 after the activation of the cAMP/PKA pathway led to polymerization of microtubules. Our study indicated that MAP2 may be a novel drug target for controlling the invasion of glioma cells.

## Materials and Methods

### *Ethics Statement*

Surgical samples were excised from glioma patients with written consent. The Sun Yat-sen University approved the protocols based on the designation of the samples as pathological waste. All animal procedures were reviewed and approved by the Ethical Committee for Use of Laboratory Animals of Sun Yat-sen University.

### *Cell Culture and Treatment*

Rat glioma cell line C6 and human glioma cell lines DBTRG-05MG and A172 were purchased from the American Type Culture Collection and maintained in Dulbecco's modified Eagle's medium (DMEM; Life Technologies) supplemented with 10% fetal bovine serum (FBS; Life Technologies) in a humidified atmosphere of 5% $CO_2$ at 37°C. Cells were maintained in DMEM containing 1% FBS (for C6) or 10% FBS (for A172 and DBTRG-05MG) when incubated with PKA activators (1 mM dbcAMP, 10 ng/mL cholera toxin, and 30 μM forskolin). The seeding density of cells and the duration of treatment are all indicated in the corresponding figure legend.

### *Human Glioblastoma Primary Cultures*

Human surgical glioma samples were obtained from the neurosurgery department of the Third Affiliated Hospital of Sun Yat-sen University. Surgical glioma explants were separated by mechanical-enzymatic digestion and centrifuged in a sterile environment. Cell pellets were then resuspended and cultured in growth medium as described above. The cells were used before passage for all experiments.

### *Scratch Wound Healing Assay*

Cells ($5 \times 10^5$) were seeded in 35 mm plates and grown to confluence, followed by drug treatment for 2 hours. Using a p200 pipette tip to scrape the cell monolayer in a straight line, a scratch wound was created in 2 perpendicular directions in the confluent cell layer. The medium and drugs were then replenished immediately, and phase-contrast images of the cells were captured 24 hours after scratching.

### *Invasion Assay*

The in vitro cell invasion assay was performed using a modified cell culture chamber (BD Biosciences Discovery Labware) with 8 μm pore size polycarbonate membrane filters. The filters were precoated with 50 μL of Matrigel (1.25 mg/mL, R&D Systems). Cells treated with drugs for 24 hours were seeded in the upper chamber at a density of $5 \times 10^4$ viable cells/well in serum-free medium, while the lower chambers were filled with culture medium supplemented with 10% FBS. Simultaneously, equivalent cells of each group were plated into 96-well plates for cell viability evaluation using 3-(4,5-dimethylthiazol-2-yl)-2,5-diphenyltetrazolium bromide (MTT; Sigma) assays. After incubation for 24 hours, the Matrigel was removed, and invaded cells were fixed with 4% paraformaldehyde/phosphate-buffered saline (PBS) for 10 minutes and stained with 0.5% crystal violet/methanol for 10 minutes. Finally, the cells were photographed and counted under a light microscope in 3-4 random fields at high power (200×). The percentage-of-invasion score was calculated as invaded cell number/total cell number × 100%.

### *MTT Viability Assay*

Cells were plated in 96-well plates and incubated overnight. After various treatments, 10 μL of MTT solution (5 mg/mL) were added and incubated for another 4 hours at 37°C. The MTT solution was removed, and 100 μL of dimethyl sulfoxide were added to dissolve the formazan crystals. The optical density (OD) was determined at 570 nm using an iMarkTM Microplate Reader (Bio-Rad). Cell viability (CV) was calculated as CV = ODexperiment/ODcontrol × 100%.

### *Confocal Microscopy*

Cells seeded on glass coverslips were exposed to different treatments and then washed, fixed, and permeabilized with 0.5%

(v/v) Triton X-100/PBS and lastly blocked with 5% (v/v) BSA/PBS for 10 minutes. Primary antibodies (mouse monoclonal anti-α-tubulin antibody, 1 : 5000 in 0.1% Triton X-100) and secondary antibodies (FITC-conjugated goat anti-mouse IgG, 1:150 in PBS) were used to examine microtubules. Pictures were captured after observation with a Zeiss (Carl Zeiss Microimaging) laser-scanning confocal microscope (LSCM).

### *Western Blotting*

Western blot was performed as described previously.[20] The following antibodies purchased from Cell Signaling Technology were used: antibodies against PKAcα (#4782), MAP2 (#8707 & #4542), STAT3 (#9139), Phospho-Stat3 (Tyr705) (#9145), c-JUN(#9165), GAPDH (#5174), and β-actin (#3700). The antibody against α-tubulin (T6074) was purchased from Sigma-Aldrich. The numbers underneath the bands in figures showing Western blotting results represent the relative protein levels quantified by measuring the grayscale of the bands using Gel Pro Analyzer (Media Cybernetics) that had been normalized to the protein levels of GAPDH or β-actin.

### *Quantitative Chromatin Immunoprecipitation Assay*

Three million cells were washed and then cross-linked with 1% formaldehyde for 10 minutes. After being washed twice with 1 mL PBS, cells were centrifuged and resuspended in 0.5 mL of lysis buffer and subsequently sonicated 15 seconds per time for 3 times . Supernatants were then recovered by centrifugation at 12 000 rpm for 10 minutes at 4°C and diluted 3 – 10 times in dilution buffer I. Ten percent of whole cell extract from each sample (input) was removed for quantitative real-time polymerase chain reaction (qPCR) before being subjected to preclearing for 2 hours at 4°C with 2 μg of sheared salmon sperm DNA, 2.5 μg of preimmune serum, and 20 μL of protein A-Sepharose. Immunoprecipitation was performed in NP-40 overnight with IgG antibodies (negative control) or anti-STAT3. Bead precipitates were then washed 3 times with TE buffer and eluted 3 times with 1% SDS, 0.1 MNaHCO3. Eluates were pooled and heated at 65°C overnight. Ten percent of the DNA preparation was used for 25 – 30 cycles of qPCR analysis after 1 hour incubation with proteinase K. p21 was used as a positive control for STAT3 occupancy.[21,22]

### *RNA Isolation, Reverse Transcription and Quantitative Real-Time PCR*

TRIzol reagent (Life Technologies) was used to isolate total RNA. SuperScript III reverse transcriptase (Life Technologies) was then used to perform reverse transcription. Thereafter, a Platinum SYBR Green qPCR SuperMix-UDG (Life Technologies) was used to perform qPCR. Primer information is provided in Supplementary Table S1.

### *Analysis of Depolymerized and Polymerized Tubulins by Immunoblotting*

Cells were collected and resuspended in 200 μL buffer (85 mM Pipes, pH 6.93; 1 mM EGTA; 1 mM $MgCl_2$; 2 M glycerol) plus 0.5% Triton X-100. After incubation (37°C, 10 min) and centrifugation

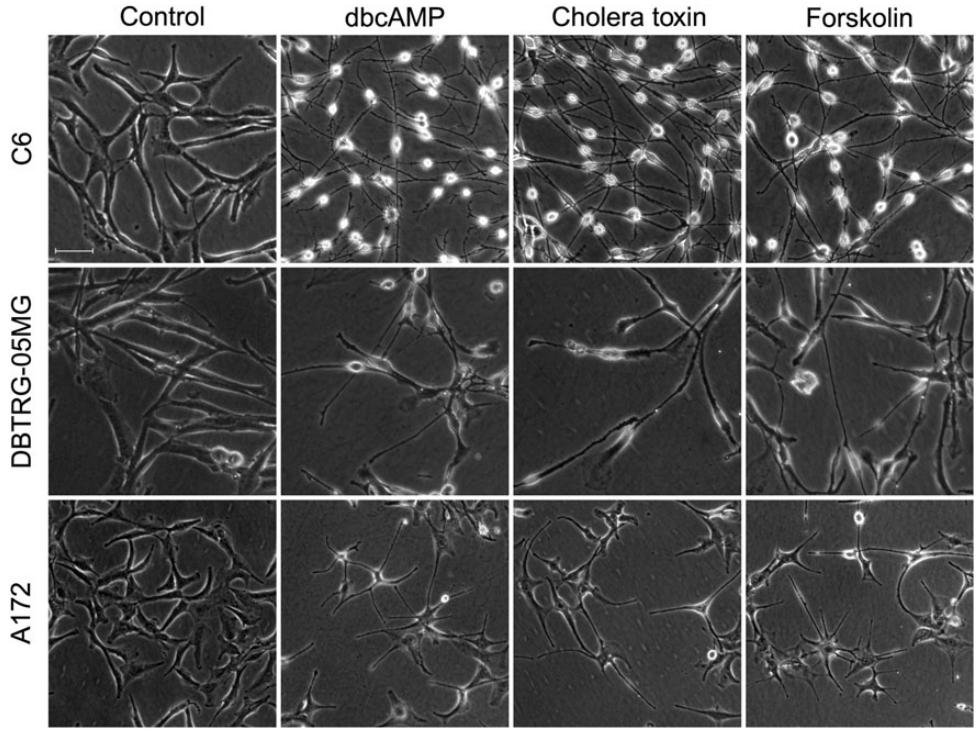


**Fig. 1.** Effects of protein kinase A (PKA) activators on the morphology of malignant glioma cells. C6, DBTRG-05MG, and A172 glioma were used to test the effects of PKA activators (1 mM dbcAMP, 10 ng/mL cholera toxin, and 30 μM forskolin). Cells ($1 \times 10^5$) were seeded in 24-well plates and incubated with different kinds of PKA activators for 48 hours (original magnification: × 100; scale bar: 100 μm).

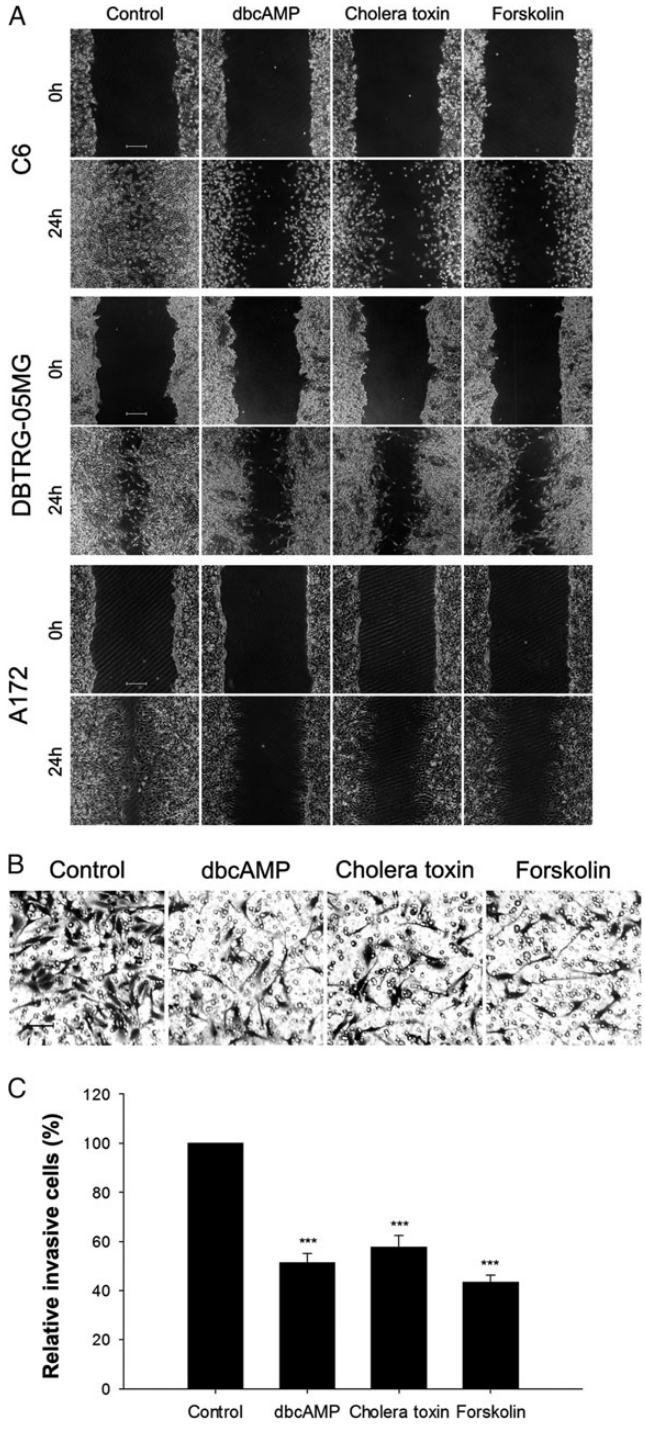


**Fig. 2.** Suppressive effects of protein kinase A (PKA) activators on migration and invasion of malignant glioma cells. (A) PKA activators (1 mM dbcAMP, 10 ng/mL cholera toxin, and 30 μM Forskolin) treatment for 48 hours significantly inhibited the migration of glioma cells, as assessed via a wound healing experiment (original magnification: ×40; scale bar: 500 μm). Cells ($5 \times 10^5$) were seeded in 35 mm plates before the wound healing experiment. (B and C). C6 glioma cells ($5 \times 10^4$) were pretreated with PKA activators (1 mM dbcAMP, 10 ng/mL cholera toxin, and 30 μM forskolin) for 24 hours and seeded into transwell inserts coated with Matrigel for an additional 24 hours. Invasive cells were counted and normalized with the number of invasive cells in the control group. The random representative fields of an experiment are shown in panel B (original magnification: × 100; scale bar: 100 μm), and the corresponding statistics are shown in panel C. Data are shown as the mean ± SD ($n = 3$). ***$P < .01$. The experiments were repeated at least 3 times before statistical analysis.

(2500 rpm, 3 min) at room temperature, depolymerized tubulins (S, in the supernatant) were separated from the polymerized tubulins (P, in the pellets). The supernatant fractions containing the depolymerized tubulins were collected, and 50 μL of 5 × SDS-PAGE gel sample buffer was added. The pellets containing the polymerized tubulins were resuspended in 250 μl microtubule stabilizing buffer (MSB) with 50 μL 5 × SDS-PAGE gel sample buffer. Then, the resulting supernatants (polymerized tubulins, P) were collected with 5 minutes boiling and 10 minutes centrifugation (14 000 rpm). Protein assays ensured that equivalent amounts of depolymerized and polymerized samples were electrophoresed and immunoblotted. Protein levels were quantitated by the integral grayscale to calculate the percentage of polymerized tubulins (determined by P[P + S]).

### *RNA Interference*

Short interfering RNA (siRNA) fragments (Ribobio) targeting the rat α isoform of the catalytic subunit of rat PKA (PKAcα), STAT3, JUN, and MAP2 transcripts were used to deplete the expressions of corresponding genes. Cells were transfected with siRNA (50 nM) by Lipofectamine RNAiMAX reagent (Life Technologies). Silencing efficiency was evaluated by Western blotting or qPCR. (See Supplementary Fig. S1A–D).

### *Statistical Analysis*

Data are presented as the mean ± SD of 3 independent experiments. Statistical analysis was performed using 1-way ANOVA, and results were considered significant if $P < .05$.

## Results

### *PKA Activators Induce Morphological Transformations of Glioma Cells*

Microscopic observation of C6, DBTRG-05MG, and A172 glioma cells treated with various PKA activators (dbcAMP, cholera toxin, and forskolin) for 48 hours revealed distinct changes in morphology compared with the control groups. Unlike the mainly polygonal morphology of the control, the PKA activator-treated cell bodies became smaller, with much longer, fine, tapering astrocyte-like processes (Fig. 1). Cell viability, as determined by the MTT assay, was similar between PKA activator-treated cells and control cells (Supplementary Fig. S2). These results were consistent with our previous results,[17–19] which indicated that PKA activators induce significant morphological changes across various glioma cell lines without noticeable decreases in cell viability.

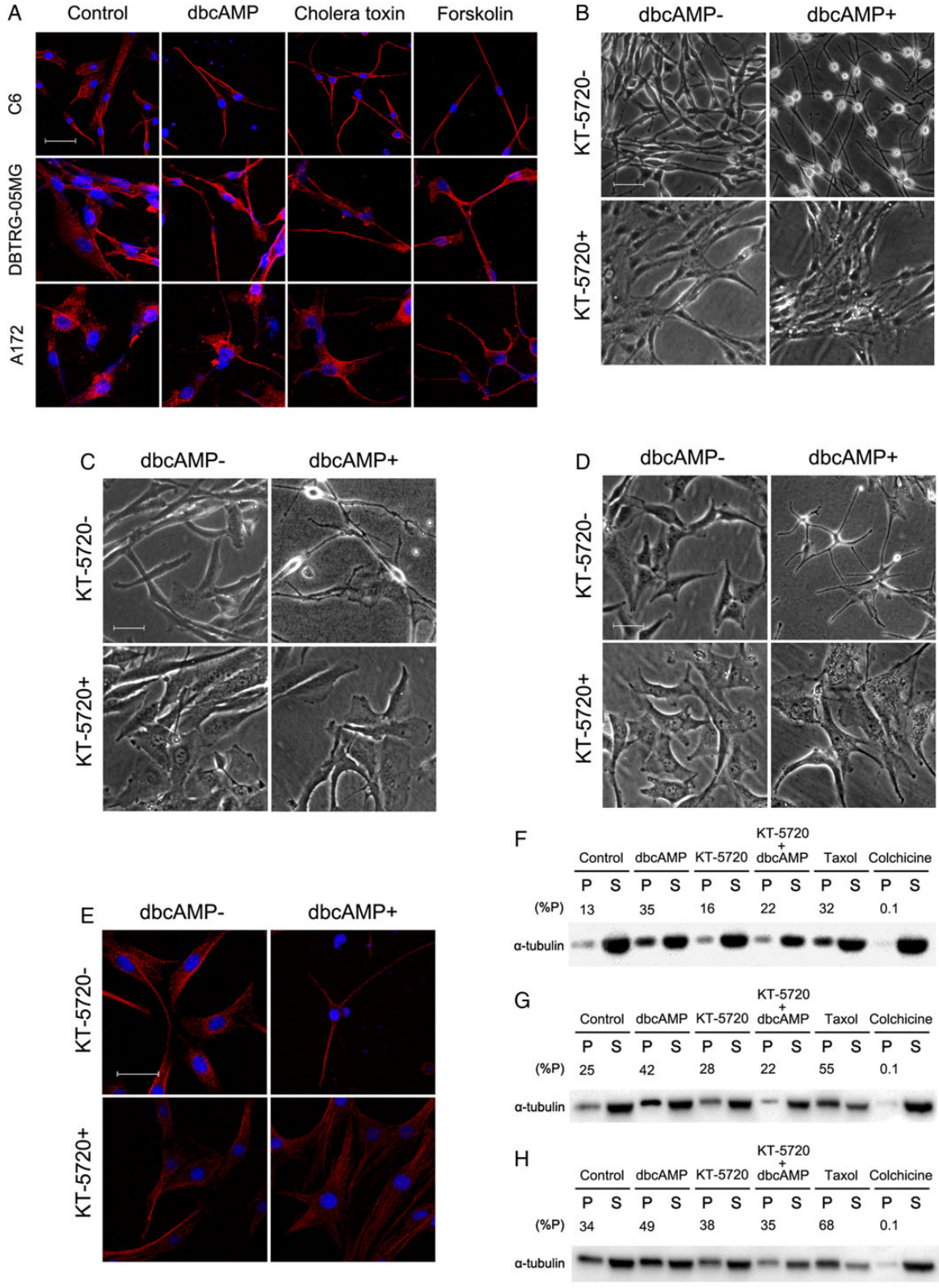


**Fig. 3.** Disruption of microtubule dynamic instability by protein kinase A (PKA) pathway. (A) Glioma cells ($2 \times 10^5$) were seeded and treated with PKA activators (1 mM dbcAMP, 10 ng/mL cholera toxin, and 30 μM forskolin) as indicated for 24 hours and then subjected to laser scanning confocal fluorescence microscopy for α-tubulin (red) and the nucleus (blue). To evaluate the role of PKA in the morphological and microtubular changes, C6 (B and E), DBTRG-05MG (C), and A172 (D) cells were seeded at a density of $5 \times 10^4$, pretreated with 2 μM PKA inhibitor KT-5720 before

### *PKA Activators Inhibit the Mobility and Invasion of Glioma Cells*

To investigate whether the morphological changes triggered by PKA activators affect the migration and invasive activity of glioma cells, wound healing and transwell assays were carried out. The wound healing assays showed that PKA activators inhibited the migratory ability of C6, DBTRG-05MG, and A172 glioma cells significantly compared with the control groups (Fig. 2A). In the transwell Matrigel invasion assay, all 3 PKA activators inhibited the invasive ability of C6 cells by more than 40% (Fig. 2B and C). These results indicated that PKA activators inhibited the migration and invasion of glioma cells without affecting their viability.

### *PKA Activation Stabilizes Cytoskeletal Microtubules in Glioma Cells*

The dynamic rearrangement of microtubules is crucial for cellular morphology and invasion. Based on the data above, we hypothesized that the PKA activators inhibit the invasion of glioma cells by disrupting the dynamics of microtubules.

Using LSCM, untreated C6, DBTRG-05MG, and A172 glioma cells showed an essentially random organization of microtubules in the cytoplasm, including a large number of microtubules radiating out from the nucleus. After treatment with PKA activators for 24 hours, the microtubules became more obvious and were well organized in the cytoplasm of the contracted cells, especially in the elongated dendrite-like protuberances (Fig. 3A). The dbcAMP-induced morphological changes of microtubules and of the whole cell could be abolished by treatment with the PKA inhibitor KT-5720 in all 3 malignant glioma cell lines (Fig. 3B–E), further indicating that the morphological changes were cAMP/PKA dependent.

To further test whether activating the cAMP/PKA pathway affects the dynamics of microtubules in glioma cells, polymerized and depolymerized tubulin contents were analyzed by Western blotting. dbcAMP considerably increased polymerized tubulins content compared with control glioma cells (Fig. 3F–H), which suggested that the microtubules were stabilized after activating the cAMP/PKA pathway. Consistent with the suggested role of the cAMP/PKA pathway in the cell morphology, KT-5720 treatment counteracted the increase in polymerized tubulin content induced by dbcAMP (Fig. 3F–H).

These results indicated that the alteration to the dynamics of microtubules induced by PKA activators triggered the morphological changes, which further inhibited the invasion and migration of glioma cells.

### *PKA Activation Upregulates MAP2 in Glioma Cells*

The MAP2 family is responsible for microtubule stabilization.[11,23,24] Low-molecular-weight MAP2 was more dramatically upregulated in response to PKA activators stimuli in C6 cells than the higher-molecular-weight MAP2 (Supplementary Fig. S3). Therefore, we focused on the role of low-molecular-weight MAP2.

After incubation with the 3 PKA activators for 48 hours, the protein levels of MAP2 were dramatically elevated in C6 cells (Fig. 4A). In addition, the induction of MAP2 by dbcAMP could also be attenuated by KT-5720 in C6, DBTRG-05MG, and A172 cells (Fig. 4B–D). SiRNA-mediated depletion of PKAcα, the catalytic subunit of PKA, also abolished the upregulation of MAP2 and the morphological changes induced by dbcAMP in C6 glioma cells (Fig. 4E and F).

These results indicated that activation of the cAMP/PKA pathway may affect the dynamics of microtubules increasing *MAP2* gene expression.

### *Transcriptional Upregulation of MAP2 Expression Is Involved in the PKA-associated Decrease in Glioma Cells' Invasion*

To further investigate how activation of the cAMP/PKA pathway upregulated *MAP2* gene expression, we used reverse transcription PCR to compare the amount of *MAP2* mRNA in glioma cells under treatment with PKA activators with that in the control cells. The levels of *MAP2* mRNA were significantly increased in C6, DBTRG-05MG, and A172 glioma cells treated with PKA activators for 24 hours (Fig. 5A). Using the transcription inhibitor actinomycin D, the increase in the MAP2 protein level induced by dbcAMP was abrogated (Fig. 5B).

We then used the University of California Santa Cruz Genome Browser (http://genome.ucsc.edu) to search the upstream regulatory sequence of the MAP2 gene and found several enriched STAT3 and JUN transcription factor-binding signals that coexist with H3K27ac and polymerase II signals (Supplementary Fig. S4), suggesting the potential involvement of these factors in the transcriptional regulation of *MAP2*. Interestingly, the interleukin 6/Janus kinase 2/STAT3 pathway is activated after cholera toxin treatment in C6 cells.[19,25] Silencing STAT3 inhibited the dbcAMP-induced upregulation of MAP2 expression (Fig. 5C, Supplementary Fig. S5). To validate that STAT3 is involved in the transcriptional upregulation of *MAP2* expression, we performed a quantitative chromatin immunoprecipitation (ChIP) assay of human glioma DBTRG-05MG cells. STAT3 could bind to the *MAP2* promoter, which was enhanced by treatment with dbcAMP (Fig. 5D). Application of the JAK2 inhibitor AG490 abolished the transcriptional elevation of *MAP2* gene expression triggered by dbcAMP (Fig. 5E).

Furthermore, depletion of *MAP2* transcripts by RNAi inhibited the morphological alterations induced by PKA activators (Fig. 5F). RNAi of *MAP2* also abolished the inhibition of human DBTRG-05MG glioma cell invasion induced by dbcAMP (Fig. 5G and H). Western blotting evaluated the silencing efficiency of *MAP2* in DBTRG-05MG cells (See Supplementary Fig. S6). Accordingly, the reduction in *MAP2* transcripts also attenuated

dbcAMP treatment for 2 hours and for an additional 48 hours with 1 mM dbcAMP. The cells were then subjected to phase contrast microscopy (B–D) or laser scanning confocal fluorescence microscopy (E) for α-tubulin (red) and the nucleus (blue) (original magnification: × 200; scale bar: 100 μm). C6 (F), DBTRG-05MG (G), and A172 (H) cells were seeded at a density of $5 \times 10^5$, treated with 1 mM dbcAMP and/or 2 μM PKA inhibitor KT-5720 to evaluate the relative abundance (%P) of polymerized tubulins (P) to total tubulins (polymerized[P] tubulins + supernatant depolymerized [S] tubulins). 50 ng/mL taxol or 1 μM colchicine was added 2 hours before the cells were harvested as the positive and negative control group, respectively.

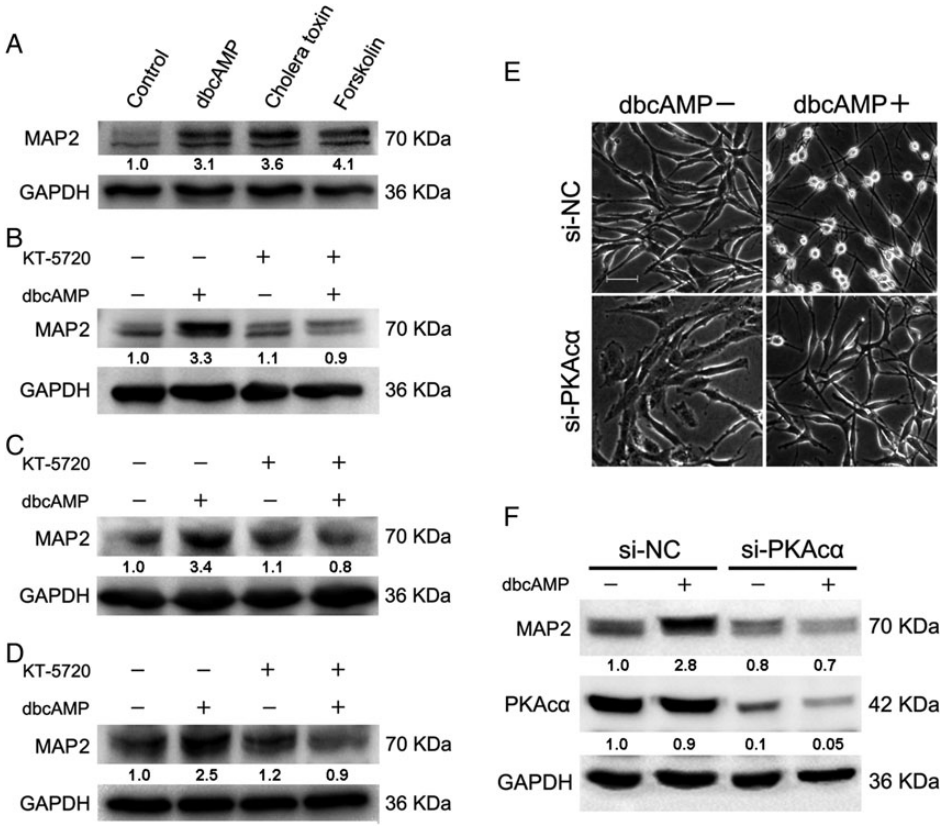


**Fig. 4.** Positive modulation of low-molecular-weight MAP2 by PKA activation. (A) C6 glioma cells were seeded at a density of $5 \times 10^5$, incubated with PKA activators (1 mM dbcAMP, 10 ng/mL cholera toxin, and 30 μM forskolin) for 48 hours, and Western blotting was then used to evaluate the protein level of low-molecular-weight MAP2. C6 (B), DBTRG-05MG (C), and A172 (D) cells were seeded at a density of $5 \times 10^5$, pretreated with 2 μM of PKA inhibitor KT-5720 for 2 hours before 1 mM dbcAMP treatment for an additional 48 hours to evaluate the protein level of MAP2. C6 glioma cells were seeded at a density of $5 \times 10^4$, transfected with 50 nM si-PKACα oligonucleotides for 24 hours, and then treated with or without 1 mM dbcAMP for an additional 48 hours to evaluate the morphological alterations (E) and MAP2 expression (F) (original magnification: × 200; scale bar: 100 μm). Antibodies were purchased from Cell Signaling Technology (#4542, #8707, #4782).

the increase in the polymerized tubulin content induced by dbcAMP (Fig. 5I).

Taken together, the results indicated that upregulation of MAP2 transcription contributes to the inhibition of glioma cell invasion.

### *PKA Activation Inhibits Invasion and Induces MAP2 Expression in Human Primary Glioblastoma Cells*

The results obtained so far implied that PKA activators induce *MAP2* expression to suppress cellular invasion in various malignant glioma cell lines. To further confirm these findings, we carried out the corresponding experiments in human primary GBM cell cultures.

Among 22 GBM cases (Supplementary table S2), the data in Fig. 6 are representative findings from one female patient's GBM cells. The patient was diagnosed with GBM based on the imaging (Supplementary Fig. S7) and molecular pathology (Supplementary Fig. S8). Similar to the findings in glioma cell lines, dbcAMP dramatically induced morphological changes in primary GBM cells, showing shrinkage of cell bodies and elongation of cellular processes. The invasiveness of the primary GBM cells was also suppressed by dbcAMP treatment in the transwell assay (Fig. 6A and B). Application of PKA inhibitor KT-5720 abolished the morphological changes induced by dbcAMP (Fig. 6C). The expression of *MAP2* was also upregulated in human primary GBM cells by treatment with dbcAMP (Fig. 6D, Supplementary Fig. S9).

## Discussion

Invasion into the adjacent normal brain tissue is one of the main features of malignant glioma. Invasive cells remaining after surgical resection are the most likely cause for the observed recurrence and death of glioma patients. Suppression of glioma invasion is an important strategy for improving the clinical outcomes of patients.

Great efforts have been made to develop cytoskeleton-disrupting drugs for cancer therapy. Typical drugs (eg, paclitaxel and docetaxel) that directly bind and stabilize microtubules—and thus trigger cell cycle arrest and apoptosis—have been used to treat different kinds of cancers.[26] Vinca alkaloids

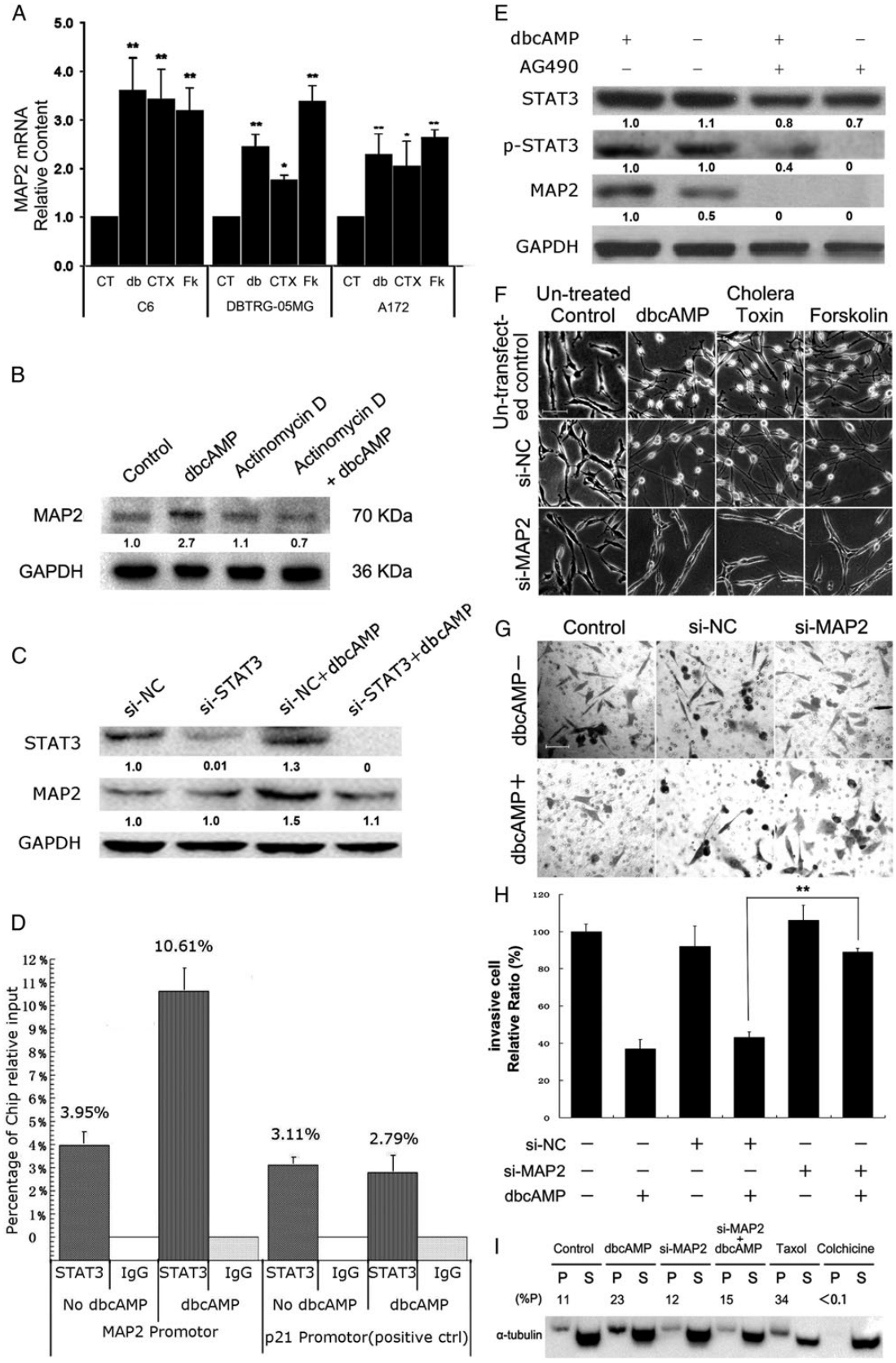
A
MAP2 mRNA Relative Content
CT db CTX Fk
C6
DBTRG-05MG
A172
B
Control
dbcAMP
Actinomycin D
Actinomycin D + dbcAMP
MAP2
70 KDa
GAPDH
36 KDa
C
si-NC
si-STAT3
si-NC+dbcAMP
si-STAT3+dbcAMP
STAT3
MAP2
GAPDH
D
Percentage of Chip relative input
3.95%
10.61%
3.11%
2.79%
STAT3
IgG
No dbcAMP
dbcAMP
MAP2 Promotor
p21 Promotor(positive ctrl)
E
dbcAMP
AG490
STAT3
p-STAT3
MAP2
GAPDH
F
Un-treated Control
dbcAMP
Cholera Toxin
Forskolin
Un-transfected control
si-NC
si-MAP2
G
Control
si-NC
si-MAP2
dbcAMP−
dbcAMP+
H
invasive cell Relative Ratio (%)
si-NC
si-MAP2
dbcAMP
I
Control
dbcAMP
si-MAP2
si-MAP2 + dbcAMP
Taxol
Colchicine
P S
(%P)
11
23
12
15
34
<0.1
α-tubulin

(including vinblastine and vincristine) also show great promise for cancer therapy. These vinca alkaloids target microtubules directly and promote depolymerization of microtubules, thus blocking mitosis and eventually leading to apoptosis.[27] However, these drugs directly targeting to the microtubules have undesired side effects. Pain and myelosuppression, which are caused by their unsatisfactory selectivity, are unfavorable for patients' quality of life. Multidrug resistance, which commonly occurs after a period of treatment, also limits their application.[12] Limitations associated with toxic side effects and drug resistance motivated us to develop alternative strategies to fight the invasion of malignant glioma.

The rapid proliferation and cellular invasion of cancer cells require active regulation of microtubules. To support rapid morphological changes, swift and stable regulation of microtubules is critical, which is controlled by MAPs that bind and help stabilize microtubules. To disrupt the polymerization dynamics of microtubules by targeting MAPs, instead of targeting the microtubules directly, may be a potential strategy for cancer therapy. In the CNS, MAP2 and Tau are the major MAPs with distinct subcellular localizations.[28,29] Tau has been found to involve axon elongation, while MAP2 plays a role in dendrite formation.[30] The MAP2 family comprises 4 isoforms (MAP2a, b, c, and d), which are produced from the same gene via alternative splicing.[8] High-molecular-weight MAP2a and 2b are responsible for dendrite stabilization, whereas low-molecular-weight MAP2c and 2d are responsible for dendrite formation and elongation.[30] Notably, defective expression of MAP2 has been observed in gliomas. Trojanowski et al demonstrated that U87, U138, U251, U373, and HS683 glioma cell lines are negative for MAP2c and MAP2d.[16]

Previously, we showed that PKA activators including cholera toxin, dbcAMP, and forskolin are capable of inducing differentiation in C6 glioma cells and human primary glioma cultures.[17,18] In addition to cell cycle arrest and potent GFAP expression, remarkable cellular morphological changes were also observed, with much longer, fine, tapering dendrite-like processes that were further confirmed in the present study (Fig. 1). Accordingly, cell invasion was suppressed by disrupting the dynamics of microtubules (Figs. 2 and 3). Low-molecular-weight MAP2 was notably induced by PKA activators, which further inhibited invasion in our models. On the other hand, suppression of *MAP2* by either blocking universal transcription with actinomycin D or specifically depleting *MAP2* mRNA by RNAi canceled the increased polymerization of microtubules, the morphological changes, and the invasion inhibition induced by activation of the cAMP/PKA pathway (Figs. 4 and 5).

The PKA-dependent MAP2 modulation presented here is somewhat different from previous findings about the relationship between these 2 components. An early study demonstrated that the modulation of MAP2 phosphorylation by PKA reduces the binding affinity of MAP2 on microtubules.[31] However, transcription-dependent modulation of MAP2 by PKA was not reported in the previous studies on the malignant glioma model. In addition, the upregulation of *MAP2* mRNA by PKA induced polymerization of microtubules and increased stability that resulted in suppression of cell invasion. Transcriptional regulation of *MAP2* has been reported in a melanoma model. Bhat et al found that Notch1 signaling-regulated HES1 represses the transcription of *MAP2* by occupying the N-box region of the *MAP2* promoter.[32] Through bioinformatic prediction, we found several enriched STAT3 and JUN binding signals coexisting with acetylated H3K27 signals and polymerase II binding signals. Using a ChIP assay and STAT3 knockdown experiments, we proved that STAT3 occupies the promoter of *MAP2* and participates in the regulation of the *MAP2* gene. RNA silencing of STAT3 inhibited dbcAMP upregulation of MAP2 expression, which suggested that STAT3 lies downstream of PKA in the MAP2 expression signaling pathway (Fig. 5C, Supplementary Fig. S5). However, whether PKA interacts with STAT3 directly or indirectly via other protein kinase (eg, Src or AMP-activated protein kinase) should be determined in a future study.[33–42] Furthermore, the detailed mechanisms of the transcriptional regulation of MAP2 in the malignant glioma model, especially in the activated PKA context, remain to be further discovered.

In summary, we report that PKA activation by PKA activators, including dbcAMP, cholera toxin, and forskolin, induce remarkable changes in the morphology of malignant glioma cell

**Fig. 5.** Transcriptional upregulation of MAP2 expression involved PKA-induced decreased invasion of glioma cells. (A) Relative mRNA levels of MAP2 were measured by quantitative real-time PCR after PKA activators (CT, control group; db, 1 mM dbcAMP; CTX, 10 ng/mL cholera toxin; Fk, 30 μM forskolin cholera toxin; Fk, 30 mM forskolin) treatment in C6, DBTRG-05MG, and A172 cells. (B) Global transcription of C6 cells was blocked by actinomycin D, and the protein level of MAP2 was measured with/without dbcAMP treatment. (C) siRNAs targeting STAT3 were transfected into C6 cells for 24 hours, followed by dbcAMP treatment for an additional 24 hours. Western blotting was used to quantify the protein level of MAP2. Cells were seeded at a density of $1 \times 10^5$. (D) After cross-linking, DNA was sonicated and immunoprecipitated at 4°C. The DNA was then extracted from the immunoprecipitate and used for quantitative real-time PCR analysis. The chromatin immunoprecipitation analysis showed STAT3 occupancy on MAP2 target promoters in DBTRG-05MG cells with or without the treatment of dbcAMP for 24 hours. The target sequences were detected by qRT-PCR analysis of eluted DNA. The relative STAT3 occupancy over the percent input is shown as a bar chart. p21 is a positive control for STAT3 occupancy. (E) DBTRG-05MG cells ($1 \times 10^6$) were seeded and pretreated with JAK2 inhibitor AG490 (12.5 μM) for 2 hours and cultured with/without 1 mM dbcAMP for 24 hours. Western blotting was used to assess the protein levels of MAP2, STAT3, and phosphorylated (Tyr705) STAT3. (F) C6 glioma ells were seeded at a density of $5 \times 10^4$. Scramble siRNA (si-NC) or siRNAs targeting MAP2 mRNA (si-MAP2) were transfected into C6 cells for 24 hours and then treated with/without PKA activators for an additional 48 hours. Untransfected controls were treated in the same way as mentioned above except without transfection of siRNA. Cellular morphological changes were examined (original magnification: × 200; scale bar: 100 μm). (G and H) DBTRG-05MG cells were seeded at a density of $5 \times 10^4$. Cell invasion of control or MAP2-silenced DBTRG-05MG cells was examined by transwell assay, as indicated, with/without 1 mM dbcAMP treatment. (original magnification: × 100; scale bar: 100 μm). (I) C6 glioma cells were seeded at a density of $5 \times 10^4$. Polymerized tubulins (named as P) in C6 cells were evaluated after MAP2 silencing for 24 hours, followed with/without an additional 48 hours of dbcAMP (1 mM) treatment. 50 ng/mL taxol or 1 μM colchicine-treated cells were harvested as the positive and negative control groups, respectively. Data are shown as the mean ± SD ($n = 3$). $^*P < .05$; $^{**}P < .01$; $^{***}P < .001$ compared with the control. The experiments were repeated at least 3 times before statistical analysis.

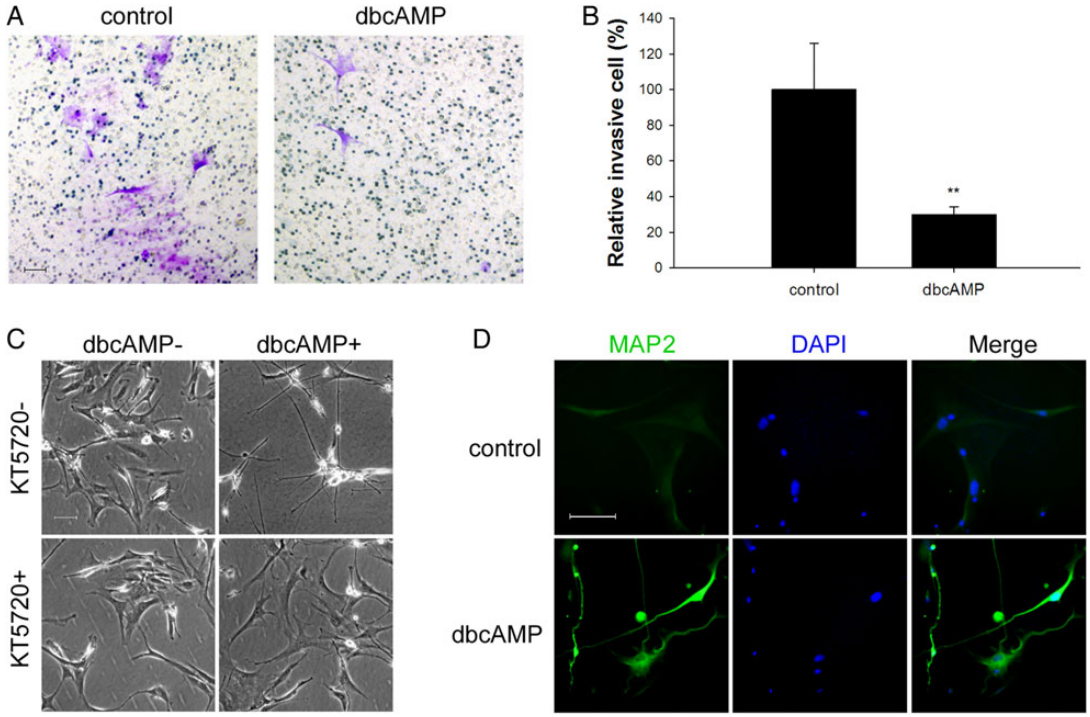


**Fig. 6.** Representative effects of dbcAMP on human glioblastoma (GBM) primary cultures. Human GBM samples were collected soon after surgery and immediately cultured. (A and B) Transwell assays were performed with primary GBM cells after 24 hours of treatment with/without dbcAMP (1 mM) as indicated. About $5 \times 10^4$ viable cells were seeded into the upper chamber. Invasive cells were counted and normalized with number of invasive cells of the control group. The random representative fields of an experiment are shown in panel A (original magnification: × 100; scale bar: 100 μm), and the corresponding statistics are shown in panel B (data are shown as the mean ± SD ($n = 3$). $^{**}P < .01$. The experiments were repeated at least 3 times before statistical analysis. (C) Cells were seeded at a density of $5 \times 10^4$and pretreated with/without 2 μM PKA inhibitor KT-5720 for 2 hours followed with/without 48 hours of treatment of 1 mM dbcAMP. Phase contrast microscopy evaluated the morphological changes (original magnification: × 100; scale bar: 100 μm). (D) Primary GBM cells were seeded at a density of $5 \times 10^4$, treated with/without 1 mM dbcAMP for 48 hours, and an immunofluorescence assay was performed to examine the expression of MAP2 (original magnification: × 200; scale bar: 100 μm).

lines and human primary GBM cells. Furthermore, the results of our experiments in cell lines and the clinical samples confirmed a mechanism shown in Supplementary Fig. S10. As can be seen in Supplementary Fig. S10, the activated PKA pathway enhances polymerization of microtubules via promoting transcription factors STAT3 involved transcription of *MAP2*, then results in the disruption of cytoskeleton dynamic instability, which lead to the inhibition of invasion at last. Our data indicate that targeting the microtubule regulation machinery, such as MAP2, may be practical for treating malignant glioma.

## Supplementary Material

Supplementary material is available online at *Neuro-Oncology* (http://neuro-oncology.oxfordjournals.org/).

## Funding

This work was supported by grants from the National Natural Science Foundation of China (Nos. 81202554, 81202555, and 81273531) and the South China Comprehensive Platform for New Medicine R&D (2009ZX09301-015).

## Acknowledgments

We thank Professor Ying Guo (the Third Affiliated Hospital of Sun Yat-Sen University) for his help in clinical specimens. We also thank Peng-Xin Qiu, Xing-Wen Su, and Jing Cai for their excellent technical assistance.

*Conflicts of interest statement.* The authors declare that they have no conflict of interest.

## References

1. Viapiano MS, Bi WL, Piepmeier J, et al. Novel tumor-specific isoforms of BEHAB/brevican identified in human malignant gliomas. *Cancer Res*. 2005;65(15):6726–6733.
2. Avgeropoulos NG, Batchelor TT. New treatment strategies for malignant gliomas. *Oncologist*. 1999;4(3):209–224.
3. Giese A, Bjerkvig R, Berens ME, et al. Cost of migration: invasion of malignant gliomas and implications for treatment. *J Clin Oncol*. 2003;21(8):1624–1636.
4. Sathornsumetee S, Rich JN. New treatment strategies for malignant gliomas. *Expert Rev Anticancer Ther*. 2006;6(7):1087–1104.

5. Nakada M, Nakada S, Demuth T, et al. Molecular targets of glioma invasion. *Cell Mol Life Sci*. 2007;64(4):458–478.
6. Dehmelt L, Halpain S. Actin and microtubules in neurite initiation: are MAPs the missing link? *J Neurobiol*. 2004;58(1):18–33.
7. Kaverina I, Straube A. Regulation of cell migration by dynamic microtubules. *Semin Cell Dev Biol*. 2011;22(9):968–974.
8. Watanabe T, Noritake J, Kaibuchi K. Regulation of microtubules in cell migration. *Trends Cell Biol*. 2005;15(2):76–83.
9. Harada A, Teng J, Takei Y, et al. MAP2 is required for dendrite elongation, PKA anchoring in dendrites, and proper PKA signal transduction. *J Cell Biol*. 2002;158(3):541–549.
10. Dehmelt L, Halpain S. The MAP2/Tau family of microtubule-associated proteins. *Genome Biol*. 2005;6(1):204–213.
11. Ludin B, Ashbridge K, Funfschilling U, et al. Functional analysis of the MAP2 repeat domain. *J Cell Sci*. 1996;109(Pt 1):91–99.
12. Cole SP, Deeley RG. Multidrug resistance mediated by the ATP-binding cassette transporter protein MRP. *Bioessays*. 1998; 20(11):931–940.
13. Dumontet C, Sikic BI. Mechanisms of action of and resistance to antitubulin agents: microtubule dynamics, drug transport, and cell death. *J Clin Oncol*. 1999;17(3):1061–1070.
14. Ernest S, Bello-Reuss E. P-glycoprotein functions and substrates: possible roles of MDR1 gene in the kidney. *Kidney Int Suppl*. 1998;65(S1):S11–S17.
15. Zientek GM, Herman MM, Katsetos CD, et al. Absence of neuron-associated microtubule proteins in the rat C-6 glioma cell line. A comparative immunoblot and immunohistochemical study. *Neuropathol Appl Neurobiol*. 1993;19(4):346–349.
16. Tlhyama T, Lee VM, Trojanowski JQ. Co-expression of low molecular weight neurofilament protein and glial fibrillary acidic protein in established human glioma cell lines. *Am J Pathol*. 1993;142(3):883–892.
17. Li Y, Yin W, Wang X, et al. Cholera toxin induces malignant glioma cell differentiation via the PKA/CREB pathway. *Proc Natl Acad Sci USA*. 2007;104(33):13438–13443.
18. He S, Zhu W, Zhou Y, et al. Transcriptional and post-transcriptional down-regulation of cyclin D1 contributes to C6 glioma cell differentiation induced by forskolin. *J Cell Biochem*. 2011;112(9): 2241–2249.
19. Shu M, Zhou Y, Zhu W, et al. Activation of a pro-survival pathway IL-6/JAK2/STAT3 contributes to glial fibrillary acidic protein induction during the cholera toxin-induced differentiation of C6 malignant glioma cells. *Mol Oncol*. 2011;5(3):265–272.
20. Umeyama T, Okabe S, Kanai Y, et al. Dynamics of microtubules bundled by microtubule associated protein 2C (MAP2C). *J Cell Biol*. 1993;120(2):451–465.
21. Barré B, Avril S, Coqueret O. Opposite regulation of myc and p21waf1 transcription by STAT3 proteins. *J Biol Chem*. 2003; 278(5):2990–2996.
22. Giraud S, Hurlstone A, Avril S, et al. Implication of BRG1 and cdk9 in the STAT3-mediated activation of the p21waf1 gene. *Oncogene*. 2004;23(44):7391–7398.
23. Ferralli J, Doll T, Matus A. Sequence analysis of MAP2 function in living cells. *J Cell Sci*. 1994;107(Pt 11):3115–3125.
24. Gustke N, Trinczek B, Biernat J, et al. Domains of tau protein and interactions with microtubules. *Biochemistry*. 1994;33(32): 9511–9522.
25. Kent WJ, Sugnet CW, Furey TS, et al. The human genome browser at UCSC. *Genome Res*. 2002;12(6):996–1006.
26. Ringel I, Horwitz SB. Studies with RP 56976 (taxotere):a semisynthetic analogue of taxol. *J Natl Cancer Inst*. 1991;83(4): 288–291.
27. Duflos A, Kruczynski A, Barret JM. Novel aspects of natural and modified vinca alkaloids. *Curr Med Chem Anticancer Agents*. 2002;2(1):55–70.
28. Boyne LJ, Martin K, Hockfield S, et al. Expression and distribution of phosphorylated MAP1B in growing axons of cultured hippocampal neurons. *J Neurosci Res*. 1995;40(4):439–450.
29. Wiche G. High-Mr microtubule-associated proteins: properties and functions. *Biochem J*. 1989;259(1):1–12.
30. Sanchez C, Diaz-Nido J, Avila J. Phosphorylation of microtubule-associated protein 2 (MAP2) and its relevance for the regulation of the neuronal cytoskeleton function. *Prog Neurobiol*. 2000; 61(2):133–168.
31. Itoh TJ, Hisanaga S, Hosoi T, et al. Phosphorylation states of microtubule-associated protein 2 (MAP2) determine the regulatory role of MAP2 in microtubule dynamics. *Biochemistry*. 1997;36(41):12574–12582.
32. Bhat KM, Maddodi N, Shashikant C, et al. Transcriptional regulation of human MAP2 gene in melanoma: role of neuronal bHLH factors and Notch1 signaling. *Nucleic Acids Res*. 2006;34(13):3819–3832.
33. Obara Y, Labudda K, Dillon TJ, et al. PKA phosphorylation of Src mediates Rap1 activation in NGF and cAMP signaling in PC12 cells. *J Cell Sci*. 2004;117(Pt 25):6085–6094.
34. Schmitt JM, Stork PJ. PKA phosphorylation of Src mediates cAMP's inhibition of cell growth via Rap1. *Mol Cell*. 2002;9(1):85–94.
35. Ram PT, Iyengar R. G protein coupled receptor signaling through the Src and Stat3 pathway: role in proliferation and transformation. *Oncogene*. 2001;20(13):1601–1606.
36. Djouder N, Tuerk RD, Suter M, et al. PKA phosphorylates and inactivates AMPKalpha to promote efficient lipolysis. *EMBO J*. 2010;29(2):469–481.
37. Damm E, Buech TR, Gudermann T, et al. Melanocortin-induced PKA activation inhibits AMPK activity via ERK-1/2 and LKB-1 in hypothalamic GT1–7 cells. *Mol Endocrinol*. 2012;26(4):643–654.
38. Nerstedt A, Johansson A, Andersson CX, et al. AMP-activated protein kinase inhibits IL-6-stimulated inflammatory response in human liver cells by suppressing phosphorylation of signal transducer and activator of transcription 3 (STAT3). *Diabetologia*. 2010;53(11):2406–2416.
39. Guo K, Ma Q, Li J, et al. Interaction of the sympathetic nerve with pancreatic cancer cells promotes perineural invasion through the activation of STAT3 signaling. *Mol Cancer Ther*. 2013;12(3): 264–273.
40. Yang Y, Pan X, Lei W, et al. Regulation of transforming growth factor-beta 1-induced apoptosis and epithelial-to-mesenchymal transition by protein kinase A and signal transducers and activators of transcription 3. *Cancer Res*. 2006;66(17):8617–8624.
41. Sriram K, Benkovic SA, Hebert MA, et al. Induction of gp130-related cytokines and activation of JAK2/STAT3 pathway in astrocytes precedes up-regulation of glial fibrillary acidic protein in the 1-methyl-4-phenyl-1,2,3,6-tetrahydropyridine model of neurodegeneration: key signaling pathway for astrogliosis in vivo? *J Biol Chem*. 2004;279(19):19936–19947.
42. Doi M, Ishida A, Miyake A, et al. Circadian regulation of intracellular G-protein signalling mediates intercellular synchrony and rhythmicity in the suprachiasmatic nucleus. *Nat Commun*. 2011; 2:327.